Research Signpost
37/661 (2), Fort P.O., Trivandrum-695 023, Kerala, India

The Nanomechanics in Italy, 2007: ISBN: 11-21 978-81-308-0237-4
Editor: Nicola Maria Pugno

2 Nanomechanics of hierarchical biomaterials

Nicola M. Pugno and Alberto Carpinteri
Department of Structural Engineering, Politecnico di Torino, Corso Duca degli Abruzzi 24, 10129 Torino, Italy

Abstract

In this Chapter two mathematical models, force- or energy-based, are proposed to design nano-bio-inspired hierarchical materials, considering strong or weak interfaces respectively. Simple formulas describing the dependence of strength, toughness and stiffness on the considered size-scale are derived, taking into account the toughening biomechanisms. A simple experimental comparison on a new two-level hierarchical grained material is also discussed.

Correspondence/Reprint request: Dr. Nicola M. Pugno, Department of Structural Engineering, Politecnico di Torino, Corso Duca degli Abruzzi 24, 10129 Torino, Italy. E-mail: nicola.pugno@polito.it

1. Introduction

Biological materials exhibit several levels of hierarchy, from the nano- to the macro-scale. For instance, sea shells have 2 or 3 orders of lamellar structures, as well as bone, similarly to dentin, has 7 orders of hierarchy [1,2]. These nano-bio-materials are composed by hard and strong mineral structures embedded in a soft and tough protein matrix. In bone and dentin, the mineral platelets are ~3nm thick, whereas in shells their thickness is of ~300nm, with very high slenderness. With this hard/soft nano-hierarchical slender texture, Nature seems to suggest us the key for optimizing materials with respect to both strength and toughness, without losing stiffness. Even if hierarchical materials are recognized to possess a fractal-like topology [3], only few engineering models explicitly considering their complex structure are present in the literature (see [4] and related references). In this Chapter an alternative and concise mathematical model is presented.

2. Strong interfaces: Force equilibrium

Strength, toughness and stiffness of materials are measured by tensile tests. Imagine a virtual tensile test on a hierarchically fibre-reinforced bar. Its cross-section, composed by hard inclusions assumed here to be perfectly embedded in a soft matrix (strong interfaces), is schematized in Figure 1.

The smallest units, at the level N, are considered scale-invariant and related to the theoretical material strengths of the hard and soft phases, respectively σ_h, σ_s, where usually $\sigma_h >> \sigma_s$. Each inclusion at the level k+1 contains n_k smaller ones, each of them with cross-sectional area A_k. Thus, the total number of inclusions at the level k is $N_k = \prod_{j=1}^{k} n_j$, having volumetric fraction $\phi_k = \prod_{j=1}^{k} \varphi_j$.

The *equilibrium equation* is $F \equiv A\sigma_C = F_h + F_s = N_k A_k \sigma_{hk} + \left(A - N_k A_k\right)\sigma_{sk} = N_N A_N \sigma_{hN} + \left(A - N_N A_N\right)\sigma_{sN}, \forall k$, where F is the critical applied force, F_h, F_s are the forces carried by the hard and soft phases respectively, $A \equiv A_0$ is the cross-section area of the bar, σ_C is its strength, $\sigma_{hN} \equiv \sigma_h$, $\sigma_{sk} \equiv \sigma_s$ ($\forall k$), and the subscript k refers to the quantities at the level k. Note that $\varphi_k = \frac{n_{k+1} A_{k+1}}{A_k}$ represents the cross-sectional fraction of the inclusions at the level k+1 in the inclusions at the level k.

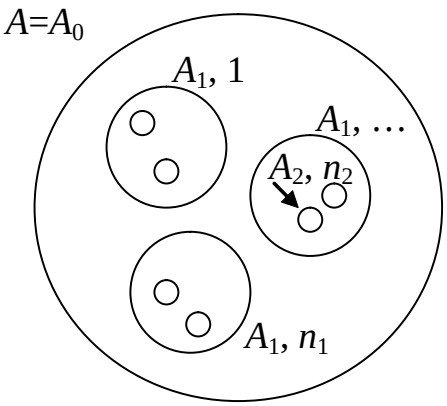

Figure 1. The cross-section of a hierarchical bar.

Natural optimization suggests nearly self-similar structures [5], for which $n_k = n$ and $\varphi_k = \varphi$, thus *k*-independent numbers and fractions; accordingly $N_k = n^k$. Since the inclusions present a fractal distribution [6], we expect $F_h \propto R^D$ where $R = \sqrt{A}$ is a characteristic size and *D* is a constant, the fractal dimension; the constant of proportionality can be deduced noting that $F_h\left(A = A_N\right) = A_N \sigma_{hN}$, and thus $F = \sigma_{hN} R_N^{2-D} R^D$. Accordingly, from $F_h = \sigma_{hN} R_N^{2-D} R^D = \sigma_{hN} n^N R_N^2$, we derive:

$$N = D \frac{\ln R/R_N}{\ln n}, \tag{1}$$

that defines the number of hierarchical levels that we need to design an object of characteristic size *R*. Eq. (1) shows that only few hierarchical levels are required for spanning several orders of magnitude in size. For example, for a nano-structured hierarchical "universe", considering for *R* its actual radius, i.e., $R \approx 10^{26}\,\mathrm{m}$, for the smallest units a radius of 1nm, i.e., $R_N \approx 10^{-9}\,\mathrm{m}$, *n*=5 and *D*=2 would result in only 100 hierarchical levels.

The scaling exponent *D* can be determined noting that $N_N A_N = A\phi$, where $\phi \equiv \phi_N = \varphi^N$ represents the macroscopic (at level 0) cross-sectional fraction of the hard inclusions. Thus, we derive $R/R_N = \left(n/\varphi\right)^{N/2}$. Introducing this result into eq. (1) provides the fractal exponent, as a function of well-defined physical quantities:

$$D = \frac{2\ln n}{\ln n - \ln \varphi}. \tag{2}$$

Note that D represents the fractal dimension of the inclusions, i.e., of a lacunar two-dimensional domain in which the soft matrix is considered as empty [7, 8]; for example, the dimension of the well-known Sierpinski carpet, is D=1.89.

Since $\sigma_{hN} n^N R_N^2 = \sigma_{hN} R_N^{2-D} R^D$ and $R/R_N = (n/\varphi)^{N/2}$, we derive:

$$\phi = \varphi^N = (R/R_N)^{D-2}. \tag{3}$$

Thus, from the equilibrium equation a scaling of the strength is predicted:

$$\sigma_C = \sigma_h \varphi^N + \sigma_s (1-\varphi^N) = \sigma_h (R/R_N)^{D-2} + \sigma_s \left(1-(R/R_N)^{D-2}\right). \tag{4}$$

Noting that $n>1$ and $\varphi<1$, we deduce $0<D<2$ and thus eq. (4) predicts that "smaller is stronger" ($\sigma_h >> \sigma_s$).

On the other hand, the *energy balance* implies $W \equiv AG_C = W_h + W_s = A_k G_{hk} + (A - N_k A_k) G_{sk} = N_N A_N G_{hN} + (A - N_N A_N) G_{sN}, \forall k$, where W, W_h, W_s are respectively the dissipated fracture energies in the bar, hard and soft phases, and G_C, $G_{hN} \equiv G_h$, $G_{sk} \equiv G_s$ ($\forall k$) are the fracture energies per unit area of the bar, hard and soft phases respectively; usually $G_h << G_s$. Accordingly, the fracture energy scales as:

$$G_C = G_h \varphi^N + G_s (1-\varphi^N) = G_h (R/R_N)^{D-2} + G_s \left(1-(R/R_N)^{D-2}\right). \tag{5}$$

And thus "larger is tougher". In the following, toughening mechanisms will be introduced in the model.

On the other hand, the *compatibility equation* implies (bars in parallel): $K \equiv EA = K_h + K_s = N_k A_k E_{hk} + (A - N_k A_k) E_{sk} = N_N A_N E_{hN} + (A - N_N A_N) E_{sN}, \forall k$, where K, K_h, K_s are respectively the "elastic" force of the bar, hard and soft phases and E, $E_{hN} \equiv E_h$, $E_{sN} \equiv E_s$ are the Young's moduli of the bar, hard and soft phases respectively. Accordingly, the Young's modulus scales as:

$$E = E_h \varphi^N + E_s (1-\varphi^N) = E_h (R/R_N)^{D-2} + E_s \left(1-(R/R_N)^{D-2}\right). \tag{6}$$

Since usually $E_h >> E_s$, "smaller is stiffer".

Eqs. (4-6) show that at the smaller size-scales the inclusions are dominating, whereas at the larger size-scales the matrix dominates. These

equations present the same self-consistent form: in fact, regarding the generic property X (σ_C, G_C or E) at the level N–1, $X_{N-1} = X_h\varphi + X_s(1-\varphi)$. Thus, at the level N–2: $X_{N-2} = X_{N-1}\varphi + X_s(1-\varphi) = X_h\varphi^2 + X_s(1-\varphi^2)$ and iterating $X \equiv X_0 = X_h\varphi^N + X_s(1-\varphi^N)$, as described by eqs. (4-6). In addition, it is clear that the scaling laws predicted by eqs. (4-6) are particularly reasonable, since they predict two asymptotic behaviours for macro- and nano size-scales. Note that for a three-dimensional architecture (i.e., particle inclusions and not longitudinal fibres) for which also the third dimension plays a role, in the stiffness of eq. (6) the factor 2 must be replaced by 3, φ becomes the volume fraction rather than the cross-sectional fraction and D is deduced from eq. (2) considering again the factor 3 instead of 2; this is true if we consider valid the rule of mixture of eq. (6) also for a nonparallel architecture.

Then, the fracture toughness can be derived as $K_C = \sqrt{G_C E}$, whereas the hardness $H \propto \sigma_C$ formally making the substitution $\sigma_C \to H$ in eq. (4). Note that the important equality (3) would allow us to derive scaling laws from "rules of mixture" also in different systems and for different properties, e.g., the friction coefficient.

Finally, for quasi-fractal hierarchy, described by $n(R)$ and $\varphi(R)$ weakly varying with the size R, a function $D(R)$ should be considered in eqs. (4-6), as deducible from eq. (2).

3. Weak interfaces: Energy balance

In the presence of weak interfaces the energy will mainly be dissipated on them during delamination, and the interfaces are thus expected to play the key role. Following [9] we assume that the dissipated energy W_{tot} is proportional to the total surface area A_{tot} of the interfaces at the fractured cross-section, and not to the nominal cross-section area A. The gain in the energy dissipation imposed by the presence of hierarchy is thus given by [10]:

$$\frac{W_{tot}-W}{W} = \frac{A_{tot}-A}{A} = \frac{2\lambda}{R^2}\sum_{k=1}^{N} N_k R_k^2 = 2\lambda\sum_{k=1}^{N}\phi_k \text{, for } \varphi_k = \varphi \Rightarrow \phi_k = \varphi^k \Rightarrow \sum_{k=1}^{N}\phi_k = \frac{\varphi-\varphi^{N+1}}{1-\varphi} \qquad (7)$$

where for spherical grains (0D) λ = 2, whereas for 1D- or 2D-inclusions $\lambda = L_k / R_k$ represents their slenderness. Note the dramatic role played by a large value of λ, as observed in the mineral platelets of nacre, bone or dentine materials, in enlarging the composite toughness. A similar mechanism is discussed in the next section for strong interfaces.

Thus, the gain in the fracture energy imposed by hierarchy (with a number of level explicitly shown here as superscripts of the symbols) is predicted to be:

$$\frac{G_C^{(N)}}{G_C^{(0)}} = 1 + 2\lambda \sum_{k=1}^{N} \phi_k \ . \tag{8}$$

For the Young's modulus, from eq. (6) we derive:

$$\frac{E^{(N)}}{E^{(0)}} = \phi_N + \frac{E_s}{E_h}\left(1 - \phi_N\right). \tag{9}$$

Thus, for the fracture toughness ($K_C = \sqrt{G_C E}$) we expect:

$$\frac{K_C^{(N)}}{K_C^{(0)}} = \sqrt{\left[1 + 2\lambda \sum_{k=1}^{N} \phi_k\right]\left[\phi_N + \frac{E_s}{E_h}\left(1 - \phi_N\right)\right]}\ . \tag{10}$$

Assuming the characteristic crack length to be proportional to $R_N^{1-2\alpha} R^{2\alpha}$ [9], where usually $0 \le \alpha \le 1/2$ (even if $\alpha > 1/2$ simply describes an inversion, often observed, of the classical Hall-Petch law), the strength $\sigma_C^{(N)} \propto K_C^{(N)} R_N^{-1/2+\alpha} R^{-\alpha}$ or hardness are predicted to be:

$$\frac{\sigma_C^{(N)}}{\sigma_C^{(0)}} = \frac{H^{(N)}}{H^{(0)}} = \left(\frac{R}{R_N}\right)^{1/2-\alpha} \sqrt{\left[1 + 2\lambda \sum_{k=1}^{N} \phi_k\right]\left[\phi_N + \frac{E_s}{E_h}\left(1 - \phi_N\right)\right]}\ . \tag{11}$$

As an example, we can treat the experimental results on double cemented WC-Co [11], a new two-level hierarchical grained material, for which $\varphi_1 = 0.73$, $\varphi_2 = 0.94$, $d_1 = 200\mu\text{m}$, $d_2 = 1 - 6\mu\text{m}$. The experimental mechanical tests were performed on standard (ASTM-B406) rectangular bars having volume V=0.500×0.625×1.875=0.586cm^3. We assume spherical grains ($\lambda = 2$). Accordingly $n_1 = \dfrac{\varphi_1 V}{\dfrac{\pi}{6} d_1^3} = 102125$ is the predicted number of mesoparticles in the total volume, whereas $n_2 = \dfrac{\varphi_2 d_1^3}{d_2^3} = 34815 - 7520000$ is that of the microparticles inside a mesoparticle. Thus the specimen is composed by several billions of microparticles. Accordint to eq. (8) the gain in

the fracture toughness energy is $\frac{G_C^{(1)}}{G_C^{(0)}} = 1 + 4\varphi_1 = 3.92$, $\frac{G_C^{(2)}}{G_C^{(0)}} = 1 + 4\left(\varphi_1 + \varphi_1\varphi_2\right) = 6.66$, thus $\frac{G_C^{(2)}}{G_C^{(1)}} = 1.70$. Assuming $E_s << E_h$, $\frac{E^{(1)}}{E^{(0)}} = \varphi_1 = 0.73$, $\frac{E^{(2)}}{E^{(0)}} = \varphi_1\varphi_2 = 0.69$ and thus $\frac{E^{(2)}}{E^{(1)}} = 0.95$. Accordingly $\frac{K_C^{(2)}}{K_C^{(1)}} = \sqrt{\frac{G_C^{(2)}}{G_C^{(1)}}\frac{E^{(2)}}{E^{(1)}}} = 1.27$, close to the experimental, even if scattered, observations [11]. Regarding the strength or hardness we expect for α = 0 (crack length proportional to the grain size) $\frac{\sigma_C^{(2)}}{\sigma_C^{(1)}} = \frac{H^{(2)}}{H^{(1)}} = \frac{K_C^{(2)}}{K_C^{(1)}}\sqrt{\frac{d_1}{d_2}} = 7 - 20$ quite unreasonable, for α = 1/2 (crack length proportional to the structural size) $\frac{\sigma_C^{(2)}}{\sigma_C^{(1)}} = \frac{H^{(2)}}{H^{(1)}} = \frac{K_C^{(2)}}{K_C^{(1)}} = 1.27$, whereas for α = 0.6 $\frac{\sigma_C^{(2)}}{\sigma_C^{(1)}} = \frac{H^{(2)}}{H^{(1)}} = \frac{K_C^{(2)}}{K_C^{(1)}}\left(\frac{d_2}{d_1}\right)^{0.1} = 0.75 - 0.89$. Since experimentally $\frac{H^{(2)}}{H^{(1)}}$ was observed to be slightly smaller than the unity, we deduce an inversion of the classical Hall-Petch law.

4. Toughening mechanisms for strong interfaces: viscoelasticity, plasticity and crack deflection or bridging

Introducing a Young's modulus we have implicitly assumed linear elasticity. For a more realistic behaviour of the matrix, we should consider visco-elasticity, often observed in bio-tissues. If $\mu_v \equiv \left(E^0 - E^\infty\right)/E^\infty$, with E^0, E^∞ short- and long-time elastic moduli respectively ($E^0 \geq E^\infty$, where the equality is valid for linear elasticity), the effective fracture energy becomes $G_s^+ = \left(1 + \mu_v\right)G_s$. The parameter μ_v represents an enhancement factor for fracture energy dissipation due to the viscoelastic properties of the medium, e.g., for bone $\mu_v \approx 4$ or for shell $\mu_v \approx 1.5$ (see [12]). Including plasticity, if μ_p represents the enhancement factor due to the plastic work during fracture $G_s^+ = \left(1 + \mu\right)G_s$, where $\mu = \mu_v + \mu_p$. The factor μ_p can be estimated for

blunt cracks as $\mu_p = \rho/(2a)$ [13], ρ being the tip radius and a being the "fracture quantum", a material/structural parameter.

According to the previous analysis and Fig. 1, the fracture surface is assumed to be planar. On the other hand, the inclusions could serve as hard structures to deflect the crack path or as crack bridging elements, assuming strong interfaces. For weak interfaces, the inclusions will be pulled-out after fracture, incrementing the dissipated energy (see previous section) in a fashion similar to the other mechanisms (if the fracture of the matrix is assumed to be similar to that of the interface; it is evident that this hypothesis can be easily removed). To model crack deflection we simply assume the two-dimensional scheme reported in Figure 2, which is a lateral view of the crack surface of Fig. 1. According to this scheme $G_s^{++} l = G_s^{+}(l + nh)$, where l is the nominal crack length, n is the number of inclusions along l and h is their height. Noting that $\varphi = nt/l$, with t thickness of the inclusions, and that $\lambda = h/t$ is their slenderness, the effective fracture energy becomes $G_s^{++} = (1 + \lambda\varphi) G_s^{+}$. Thus, also this toughening mechanism can enhance the effective fracture energy G_s^{++} ($\mu \approx \varphi \approx 1; \lambda >> 1$) by several orders of magnitude with respect to the intrinsic fracture energy of the matrix G_s. This explains why the shape of mineral crystals is found to be very anisometric (platelets, [12]), no matter if the interfaces are strong or weak: the anisometry is larger for bone and dentin (platelets 3nm thick and up to 100nm long) as well as for enamel (15-20nm thick, 1000nm long) than for nacre (i.e., see shells, 200-500nm thick and 5-8μm long). For details on the hierarchical bone structure see [14]. Thus, eq. (5) has in general to be considered with the substitutions:

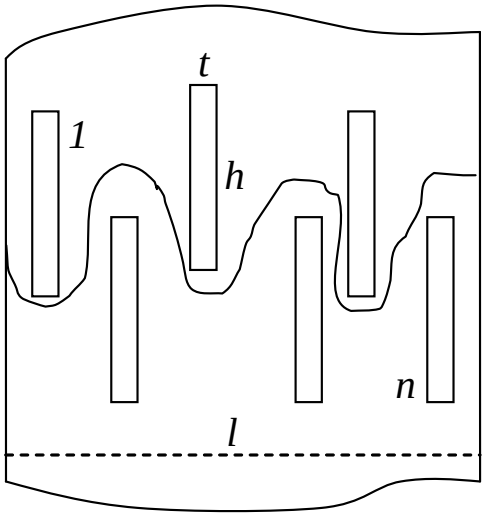

Figure 2. The lateral view of the crack surface: toughening mechanisms.

$$G_s \to (1+\mu)(1+\lambda\varphi)G_s \tag{12a}$$

$$G_h \to 0 \tag{12b}$$

since in this case no dissipation occurs in the hard phase.

Furthermore, a soft matrix activates shear mechanisms rather than longitudinal ones, according to the tension-shear chain model recently proposed [12]. Since in this case matrix does not carry tensile load, the substitution:

$$\sigma_s \to 0 \tag{13}$$

should be considered in eq. (4). Considering a linear variation of the shear stress (but stress concentration factors could be included [15]) with a maximum value τ implies a maximum normal stress σ in the platelet equal to $\lambda\tau$ [12]. Thus, load transfer requires $\lambda\tau_s > \sigma_C$ where τ_s is the shear strength of the matrix (or, strictly speaking, of the matrix/inclusion interface); this shows that low values of τ_s are compensated in Nature by high slendernesses λ. Note that according to [12] an in-series tension/shear rather than an in-parallel tension architecture, as considered in eq. (6), emerges. However, their asymptotic behaviours (for realistic sufficiently large size-scales R) are identical if in eq. (6) the Young's modulus of the matrix is assumed to be negligible, i.e.:

$$E_s \to 0 \tag{14}$$

5. Size and shape of "flaw-tolerant" 1D- 2D-inclusions

Let us consider for the sake of simplicity the Griffith's problem. According to Quantized Fracture Mechanics [13] the failure stress is predicted to be $\sigma_f = \sqrt{G_C E/(\pi l + a/2)}$, where $2l$ is the crack length and a is the fracture quantum (Linear Elastic Fracture Mechanics, LEFM, assumes a=0). Thus, a "flaw tolerance" is expected to take place for crack lengths $2l$ smaller than a and surely in platelets with thickness $t \approx a$. The fracture quantum a can be estimated noting that $\sigma_f(l=0) = \sigma_C$ and thus the platelet thickness or grain size for flaw tolerance is:

$$t_N \approx \frac{G_C^{(N)} E^{(N)}}{\sigma_C^{(N)2}} \tag{15}$$

similarly to what previously deduced [16, 12]. This characteristic length represents also the optimal diameters for hierarchical grains (or grain size). Inserting eqs. (4), (5) and (6) or (8), (9) and (11) into eq. (15) defines the thicknesses of the inclusions at all the hierarchical levels for flaw tolerance.

In addition, to reach the failure simultaneously in the soft and hard phases, the following equation for the slenderness at a given hierarchical level must hold (see previous section):

$$\lambda_N \approx \sigma_C^{(N)} / \tau_s \tag{16}$$

Finally, Nature seems to optimize structures by imposing the ratio between fractal D and Euclidean nominal dimensions D according to $D/\mathrm{D}=\mathrm{D}/(\mathrm{D}+1)$ [17], e.g., for D=3, $D/3=3/4$ [5]. Thus $D/2 \approx 2/3$, and, from eq. (2), the optimum would imply:

$$D_{opt} \approx 4/3, \quad \text{or,} \quad \left(\varphi n^{1/2}\right)_{opt} \approx 1 \tag{17}$$

The fractal dimension of the inclusions, according to eq. (17), is intermediate between those of an Euclidean line and surface.

Eq. (15) defines the optimal platelet thicknesses for flaw tolerant, eq. (16) the optimal platelet slenderness to have a uniform strength in both the phases and eq. (17) the relation between their number and cross-sectional area fraction for having an optimal fractal dimension.

6. Conclusions

The developed mathematical model, summarized in the numbered equations, allows us to preliminary design nano-bio-inspired hierarchical materials, by following a bottom-up or top-down procedure. The complexity of the problem has imposed a simplified treatment with associated limitations; nevertheless, the model could be useful for preliminary designing micro- or nano-structured hierarchical materials.

Acknowledgement

The authors are supported by the ‘‘Bando Ricerca Scientifica Piemonte 2006’’ – BIADS: Novel biomaterials for intraoperative adjustable devices for fine tuning of prostheses shape and performance in surgery.

References

1. J. D. Currey 1977 *Proceedings of the Royal Society* B **196** 443.
2. J. D. Currey 1984 *The Mechanical Adaptations of Bones* (Princeton, NJ, Princeton University Press) pp. 24-37.
3. R. Lakes 1993 *Nature* **361** 511.

4. H. Gao 2006 *International Journal of Fracture* **138** 101.
5. J. H. Brown and G. B. West 1999 *Scaling in biology* (Oxford University Press, Oxford).
6. A. Carpinteri and N. Pugno 2005 *Nature Materials* **4** 421.
7. A. Carpinteri 1994 *Mechanics of Materials* **18** 89.
8. A. Carpinteri 1994 *International Journal of Solids and Structures* **31** 291.
9. A. Carpinteri and N. Pugno 2005 *Review on Advanced Material Science Journal* **10** 320.
10. N. Pugno 2007 *J Physics – Cond. Matt* 19 395001 (17pp).
11. Z.Z. Fang, A. Griffo, B. White, G. Lockwood, D. Belnap, G. Hilmas and J. Bitler 2001 *Int. J. Refractory Metals and Hard Materials* **19** 453.
12. B. Ji and H. Gao 2004 *Journal of the Mechanics and Physics of Solids* **52** 1963.
13. N. Pugno and R. Ruoff 2004 *Philosophical Magazine* **84** 2829.
14. O. Akkus, Y.N. Yeni and N. Wesserman 2004 *Critical Reviews in Biomedical Engineering* **32** 379.
15. N. Pugno and A. Carpinteri 2003 *Journal of Applied Mechanics* **70** 832.
16. A. Carpinteri 1982 *Engineering Fracture Mechanics* **16** 467.
17. R.B. Banavar, A. Maritan and A. Rinaldo 1999 *Nature* **399** 130.